



Properties and pharmacological modification of ATP-sensitive K^+ channels in cat tracheal myocytes

*¹Noriyoshi Teramoto, ¹Tadasu Nakashima & ¹Yushi Ito

¹Department of Pharmacology, Graduate School of Medical Sciences, Kyushu University, Fukuoka, 812-8582, Japan

1 The effects of levcromakalim and nucleoside diphosphates (NDPs) on both membrane currents and unitary currents in cat trachea myocytes were investigated by use of patch-clamp techniques.

2 In conventional whole-cell configuration, levcromakalim produced a concentration-dependent K^+ current which was suppressed by additional application of 5 μM glibenclamide at -70 mV. When 3 mM ATP was added in the pipette solution, the peak amplitude of the levcromakalim-induced current was much smaller than that in the absence of ATP.

3 When 3 mM uridine 5'-diphosphate (UDP) was included in the pipette solution, much higher concentrations of glibenclamide (≥ 50 μM) were required to suppress the 100 μM levcromakalim-induced membrane current in comparison with those in the absence of UDP.

4 In the cell-attached patches, levcromakalim activated a 40 pS K^+ channel which was inhibited by additional application of glibenclamide in symmetrical 140 mM K^+ conditions.

5 UDP (≥ 0.1 mM) was capable of reactivating the channel in inside-out patches in which the glibenclamide-sensitive K^+ channel had run down, in the presence of levcromakalim. The K^+ channel reactivated by UDP was suppressed by additional application of either intracellular 3 mM ATP or 100 μM glibenclamide.

6 These results demonstrate that smooth muscle cells in the cat trachea possess ATP-sensitive 40 pS K^+ channels which are blocked by glibenclamide (i.e. K_{ATP}) and can be activated by levcromakalim and that intracellular UDP causes a significant shift of the glibenclamide-sensitivity of these channels.

British Journal of Pharmacology (2000) **130**, 625–635

Keywords: ATP-sensitive K^+ channels; glibenclamide; glibenclamide-sensitivity; levcromakalim; nucleoside diphosphates

Abbreviations: ADP, adenosine 5'-diphosphate; ANOVA, analysis of variance; E_K , theoretical potassium equilibrium potential; GDP, guanosine 5'-diphosphate; K_{ATP} , ATP-sensitive 40 pS K^+ channels; K_{ir} , inward-rectifying K^+ channel; NBFs, nucleotide-binding folds; NDPs, nucleoside diphosphates; NP_o , channel open state probability; PSS, physiological salt solution; SUR, sulphonylurea receptor; TEACl, tetraethylammonium chloride; UDP, uridine 5'-diphosphate

Introduction

K^+ channels inhibited by intracellular ATP have been identified in a wide variety of tissues, and are referred to as ATP-sensitive K^+ channels (K_{ATP}). It is well-known that K_{ATP} play an important role in regulating not only the resting membrane potential but also the membrane excitability (reviewed by Edwards & Weston, 1993). As these channel activities are also regulated by intracellular nucleoside diphosphates (NDPs), they have been termed NDP-sensitive K^+ channels in smooth muscle (Quayle *et al.*, 1997).

In airway smooth muscle, since glibenclamide selectively inhibits not only the membrane hyperpolarization (Murray *et al.*, 1989), but also the K^+ ($^{86}Rb^+$) efflux (Allen *et al.*, 1986) and the muscle relaxation induced by K^+ channel openers (guinea-pig, Arch *et al.*, 1988; human, Black *et al.*, 1990), it is generally believed that glibenclamide-sensitive K^+ channels are the target channels for K^+ channel openers. Recently, Nuttle & Farley (1997) have reported that in swine cultured tracheal smooth muscle cells, (\pm)-cromakalim-induced glibenclamide-sensitive membrane currents are inhibited by protein kinase C through muscarinic receptors. However, there has been no direct report concerning the electrophysiological and pharmacological properties of the glibenclamide-sensitive K^+ channels in tracheal myocytes by use of single-

channel recordings. Furthermore, the effects of NDPs on membrane currents still remain to be evaluated in these cells, although NDP-sensitivity is one of the most important characteristics of K_{ATP} in other smooth muscle (Quayle *et al.*, 1997). Thus, it is of importance to investigate the effects of K^+ channel openers and NDPs on the unitary currents in airway smooth muscle cells. The present study was designed to elucidate the effects exerted by levcromakalim and NDPs on both macroscopic and unitary currents in freshly dispersed cat tracheal myocytes. In addition, we have studied the effects of NDPs on the sensitivity of K_{ATP} to glibenclamide.

Methods

Adult mongrel cats of either sex weighing 3–4 kg were anaesthetized with intramuscular sodium pentobarbitone and then killed by exsanguination. A segment of cervical trachea (5–6 cm) was excised and quickly transferred into modified Krebs solution aerated with 95% O_2 and 5% CO_2 . After removing attached connective tissue from its outer surface (the cartilage was left attached to keep tension on the muscle), the segment was allowed to fully relax in modified Krebs solution under oxygenated conditions at room temperature (22–25°C), an equilibration procedure, which normally required 2–3 h.

*Author for correspondence;

E-mail: noritera@linne.med.kyushu-u.ac.jp

Cell dispersion

The procedures used to disperse the smooth muscle cells were similar to those reported previously (Waniishi *et al.*, 1998). Briefly, the above relaxed segment was incubated in modified Krebs solution (1.5 mM Ca^{2+} present) containing collagenase (Sigma type I, 2.0–2.5 mg ml⁻¹) and protease (Sigma, 0.1–0.2 mg ml⁻¹), for 40–45 min at 36–37°C. Relaxed spindle-shaped cells, with length varying between 400 μ m and 500 μ m, were isolated by the gentle tapping method (Teramoto & Brading, 1996) and stored at 4–5°C. All experiments were performed at room temperature (22–25°C).

Solutions and drugs

The composition of solutions used was as follows (mM): modified Krebs solution; Na^+ 137, K^+ 5.9, Mg^{2+} 1.2, Ca^{2+} 1.5, HCO_3^- 15.5, $H_2PO_4^-$ 2.5, Cl^- 130.3, glucose 12; physiological salt solution (PSS); Na^+ 140, K^+ 5, Mg^{2+} 1.2, Ca^{2+} 2, glucose 5, Cl^- 151.4, HEPES 10, titrated to pH 7.35–7.40 with Tris base; pipette solution (mM): K^+ 140, Cl^- 140, EGTA 5, HEPES 10/Tris (pH 7.35–7.40). ATP or NDPs were occasionally included in the pipette solution as indicated in the results section. For single-channel recordings, the pipette and bath solution was high potassium solution (mM): K^+ 140, Cl^- 140, EGTA 5, Glucose 5, HEPES 10/Tris (pH 7.35–7.40) producing symmetrical 140 mM K^+ conditions. Cells were allowed to settle in the small experimental chamber (approximately 80 μ l in volume). The bath solution was superfused by gravity throughout the experiments at a rate of 2 ml min⁻¹. For rapid drug application we used the flowing solution system

(a concentration jump technique, Teramoto & Brading, 1996), recording the drug application time as a trigger pulse on VHS tape with current and voltage at the same time. The following chemicals were used: ATP, adenosine 5'-diphosphate (ADP), guanosine 5'-diphosphate (GDP), uridine 5'-diphosphate (UDP), HEPES (all chemicals were obtained from Sigma). Levromakalim was kindly provided by SmithKline Beecham Pharmaceuticals (Harlow, U.K.). Levromakalim and glibenclamide were prepared daily as 100 mM stock solutions in DMSO. The final concentration of DMSO was less than 0.1%, and this concentration was shown not to affect K^+ current in cat trachea.

Electrophysiology

The experimental system used was essentially the same as that described previously (Teramoto *et al.*, 1999). Generation of voltage pulses was performed using a L/M-EPC 8 patch-clamp amplifier (HEKA Elektronik Corp., Lambrecht, Germany) in conjunction with a circuit board which has both an analogue to digital and a digital to analogue conversion function (ITC-16, Instrutech Corp., NY, U.S.A.), using a 'Pulse' software package (HEKA Elektronik Corp., Lambrecht, Germany). The sampled current data were filtered at 10 kHz and stored together with potential records on videotape using a digital data recorder (VR-10B, Instrutech Corp., NY, U.S.A.) coupled to a video recorder (Panasonic, Tokyo, Japan) for subsequent off-line analysis. Junction potentials between bath and pipette solutions were measured using a 3 M KCl reference electrode and were <2 mV, so that correction for these potentials was not made. Capacitance noise was kept to a

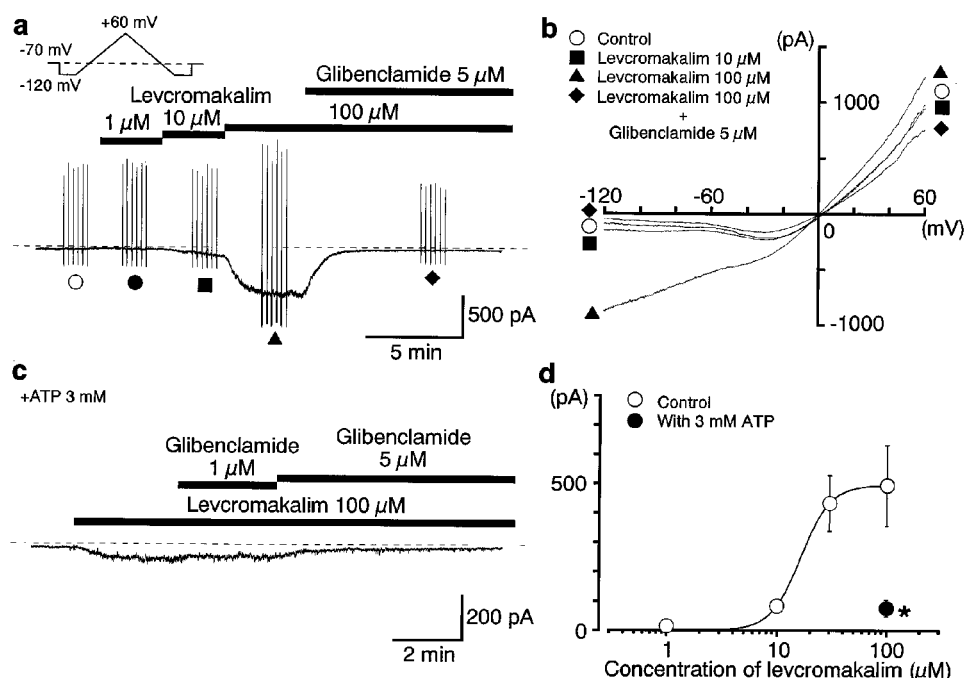


Figure 1 Levromakalim-induced membrane current in symmetrical 140 mM K^+ conditions recording from single-isolated smooth muscle cells of cat trachea by use of a conventional whole-cell configuration at a holding potential of -70 mV. (a) A cumulative application of levromakalim caused a concentration-dependent inward current at -70 mV. The vertical deflections indicate triangle ramp potential pulses (see inset, every 15 s) in the absence and presence of levromakalim. The dashed line indicates the zero current level. (b) The mean ramp membrane currents on an expanded time scale in each condition. Symbols as in (a). (c) Effects of 100 μ M levromakalim on the membrane current when the pipette solution contained 3 mM ATP. Dashed line: zero current level. (d) Relationships between peak amplitude of inward currents and concentration of levromakalim in the absence and presence of ATP (3 mM) in the pipette solution. The peak amplitude of the levromakalim-induced currents were measured from the 5 μ M glibenclamide-sensitive level in each condition. Each symbol indicates mean and s.d. of 8–10 observations.

minimum by maintaining the test solution in the electrode as low as possible. At the beginning of each experiment, the series resistance was compensated.

Data analysis

The whole-cell current data were low-pass filtered at 500 Hz by an 8 pole Bessel filter, sampled at 25 ms and analysed on a computer (Macintosh G3, Apple Computer Japan Ltd, Tokyo, Japan) by the commercial software 'MacLab 3.5.6' (ADInstruments Pty Ltd, Castle Hill, Australia). For single-channel recordings, the stored data were low-pass filtered at 2 kHz (−3 dB) and sampled into the computer with a digitalized interval of 50 μ s using 'Patch Analyst Pro version 1.21' (MT Corp., Tokyo, Japan); events briefer than 50 μ s were not included in the evaluation. The all-point amplitude histogram was obtained from a continuous recording of 1 or 2 min (2 kHz filtration; 50 μ s digital sampling interval), and fitted with the Gaussian distribution function using a least-squares fitting. Continuous traces in the figures were obtained from records filtered at 500 Hz for presentation (digital sampling interval, 25 ms). Data points were fitted using a least-squares fitting.

Statistics

Statistical analyses were performed with either Student's *t*-test for paired values or analysis of variance (ANOVA) test (two-

factor with replication). Changes were considered significant at $P < 0.01$. Data are expressed as mean with the standard deviation (s.d.).

Results

Levcromakalim-induced glibenclamide-sensitive current in cat tracheal myocytes

When the pipette solution was filled with 140 mM KCl solution containing 5 mM EGTA and the bath solution was superfused by 140 mM K⁺ PSS (symmetrical 140 mM K⁺ conditions) at a holding potential of −70 mV in a conventional whole-cell configuration, application of levcromakalim (≥ 10 μ M) caused a significant inward current in cat tracheal myocytes (Figure 1a). When the concentration of levcromakalim was increased in a cumulative manner (from 1 μ M to 100 μ M), the peak amplitude of the levcromakalim-induced basal membrane current at −70 mV increased in a concentration-dependent manner (Figure 1a,d). Subsequent application of 5 μ M glibenclamide suppressed the levcromakalim-induced current to the control level. Before and during application of each concentration of levcromakalim, current-voltage (*I*-*V*) relationships were obtained by applying six ramp pulses (from −120 mV to +60 mV for 900 ms duration) every 15 s at −70 mV (Figure 1b). When 3 mM ATP was added to the pipette solution, the peak amplitude of the levcromakalim

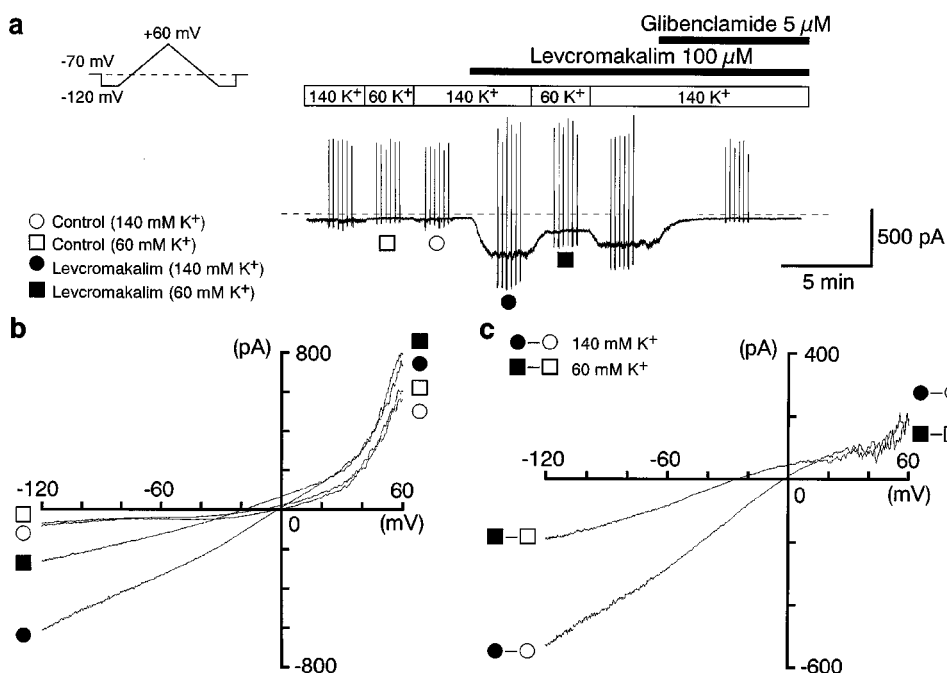


Figure 2 The levcromakalim-induced membrane current is mainly a K⁺ current due to increased K⁺ permeability in cat tracheal myocytes. Holding potential was kept at −70 mV. Bath solution was initially 140 mM K⁺ PSS, and [K⁺]_o was transiently reduced from 140 mM K⁺ to 60 mM K⁺. Pipette solution was 140 mM KCl containing 5 mM EGTA. Similar observations were obtained in six other cells. Data were sampled at 25 ms (continuous traces) or 1 ms (ramp currents). (a) Ramp currents induced by the six ramp potential pulses from −120 mV to 60 mV for 900 ms after a 300 ms conditioning pulse (−120 mV, see inset) applied every 15 s before and during application of 100 μ M levcromakalim. In the absence of levcromakalim (control), the ramp membrane currents were obtained in either 140 mM K⁺ condition or 60 mM K⁺ condition. Levcromakalim (100 μ M) caused an inward current in symmetrical 140 mM K⁺ conditions. In the presence of levcromakalim, the same voltage protocol was performed. When [K⁺]_o was reduced from 140 mM to 60 mM, the peak amplitude of the basal sustained levcromakalim-induced current decreased at −70 mV. The vertical deflections indicate ramp currents. The dashed line indicates the zero-current level. (b) The mean ramp membrane currents on an expanded time scale in several conditions. Each symbol is the same as in (a). (c) Net membrane current evoked by levcromakalim (100 μ M) when [K⁺]_o was either 60 mM or 140 mM. Net membrane current was obtained by subtraction of the two ramp membrane currents (shown in b) recorded before and during application of 100 μ M levcromakalim in each [K⁺]_o conditions. The reversal potential of levcromakalim-induced current in 140 mM K⁺ was −3 mV. The reversal potential in 60 mM K⁺ was −23 mV.

(100 μ M)-induced current was much smaller (76 ± 29 pA, $n = 8$ with ATP *versus* 494 ± 138 pA, $n = 8$ without ATP). This small inward current was also suppressed by additional application of 5 μ M glibenclamide (Figure 1c). Figure 1d summarizes the relationship between the peak amplitude of the inward current and the concentration of levcromakalim in the absence and presence of intracellular ATP. To make a rough estimation of the ion selectivity and the reversal potential of this current, voltage ramps were applied (see inset in Figure 2a) and the extracellular K⁺ concentration ($[K^+]_o$) was changed by isosmotic substitution of Na⁺. Figure 2a shows the experimental protocol. In the absence of levcromakalim (control), *I-V* relationships were obtained by the application of six ramp pulses in solutions containing 140 mM K⁺ PSS followed by 60 mM K⁺ PSS and then back to 140 mM K⁺ PSS. Levcromakalim (100 μ M) was then applied in the bath solution and caused a sustained inward current; the same voltage protocol was then performed. When $[K^+]_o$ was decreased from 140 mM to 60 mM, the sustained levcromakalim-induced membrane current at -70 mV was decreased. When $[K^+]_o$ was returned to 140 mM, the amplitude of the levcromakalim-induced sustained current became larger, however did not restore towards the original level. Figure 2b shows the average of the six ramp currents before and during the application of 100 μ M levcromakalim for the cell shown in Figure 2a. In each

$[K^+]_o$ condition, the net membrane current activated by 100 μ M levcromakalim was obtained by subtracting the averaged control current from the mean levcromakalim-induced current. The current demonstrated an inwardly rectifying property (Figure 2c). The reversal potential of the levcromakalim-induced membrane current in this cell was -3 mV in 140 mM K⁺ (-2 ± 3 mV, $n = 6$) and -23 mV in 60 mM K⁺, (-24 ± 2 mV, $n = 6$). Note that n represents not the number of the ramped voltage commands from the one cell but the number of cells. These values were close to the theoretical potassium equilibrium potential (E_K) in each $[K^+]_o$ condition (140 mM K⁺; $E_K = 0$ mV, 60 mM K⁺; $E_K = -21$ mV). These results suggest that in cat tracheal myocytes, the levcromakalim-induced membrane currents are carried mainly by K⁺ through channels that are sensitive to glibenclamide.

Pharmacological characterization of the levcromakalim-induced inward current in cat trachea

The effects of Ba²⁺ and TEA⁺ on the levcromakalim-induced currents were studied in symmetrical 140 mM K⁺ conditions at -70 mV. Figure 3a shows an example of the inhibitory effects of Ba²⁺ and glibenclamide on the current in the same cell. The time course of the inhibitory action of Ba²⁺ and glibenclamide

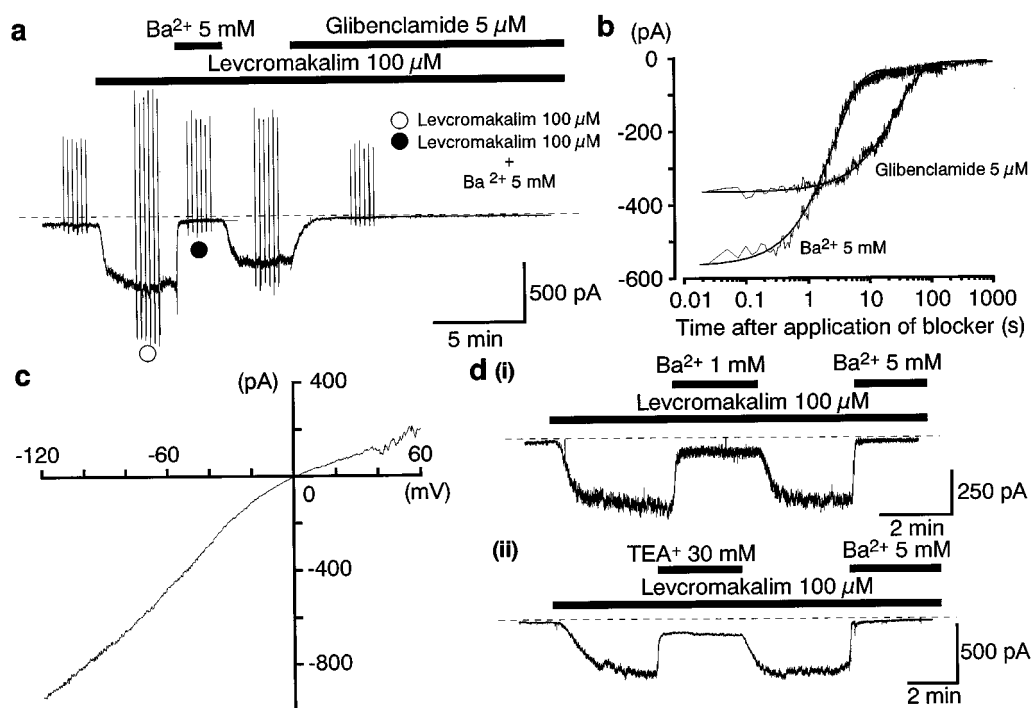


Figure 3 Inhibitory kinetics of glibenclamide, Ba²⁺ and TEA⁺ on the 100 μ M levcromakalim-induced inward current at -70 mV. The bath was 140 mM K⁺ PSS and the pipette was 140 mM KCl containing 5 mM EGTA (i.e., symmetrical 140 mM K⁺ conditions). (a) Inhibitory effects of 5 mM Ba²⁺ and 5 μ M glibenclamide. A single exponential (solid line) was fitted to the current decay from time zero (start of application of each blocker).

$$I(t) = I_o + I_a \exp(-t / \tau_a)$$

$I_o = -45$ pA, $I_a = -527$ pA and $\tau_a = 6$ s, (5 mM Ba²⁺) and $I_o = -13$ pA, $I_a = -352$ pA and $\tau_a = 47$ s, (5 μ M glibenclamide), respectively. The dashed line indicates the zero current level. (b) The expanded fitting trace of the Ba²⁺ and glibenclamide-induced inhibitory time courses. The solid line indicates the exponential fitting. The time 0 indicates the time when each blocker was applied by a concentration jump method. The abscissa scale shows the amplitude of the inward current (pA) and the ordinate scale shows the duration of application of glibenclamide (min) in a logarithmic scale. The membrane current was filtered through 2 kHz and the duration of the sampling time was 25 ms. (c) Difference between the mean levcromakalim-induced membrane current in the presence and absence of 5 mM Ba²⁺. Net membrane current (Ba²⁺-sensitive current) was obtained by subtraction of the two ramp membrane currents recorded before and during application of 5 mM Ba²⁺ when 100 μ M levcromakalim was present in the bath. (d) Effects of Ba²⁺ (1, 5 mM) (i) and TEA⁺ (30 mM) (ii) on the levcromakalim-induced membrane current at -70 mV. The dashed line indicates the zero current level.

on the levcromakalim-induced current was evaluated by plotting the current amplitude against the time after application of each blocker in a single exponential fitting (Figure 3b), and the mean inhibitory time constant was 5 ± 2 s (Ba^{2+} , $n=6$), and 45 ± 4 s (glibenclamide, $n=6$), respectively. Figure 3c demonstrates the net membrane current obtained by subtraction of the two mean ramp currents recorded before and during application of Ba^{2+} in the presence of $100 \mu\text{M}$ levcromakalim, demonstrating a significant inwardly rectification at positive potentials. Figure 3d shows that Ba^{2+} inhibited the levcromakalim-induced membrane current in a concentration-dependent manner. When the peak amplitude of the levcromakalim-induced current at -70 mV was normalized as 1.0, the relative inhibitory ratio of Ba^{2+} , measured from the current level of $5 \mu\text{M}$ glibenclamide, was $20 \pm 7\%$, $n=5$, (1 mM Ba^{2+}) and $6 \pm 2\%$, $n=6$, (5 mM Ba^{2+}). Application of 30 mM

tetraethylammonium chloride (TEACl) also inhibited the levcromakalim-induced current at -70 mV ($22 \pm 5\%$, $n=5$), however, the inhibitory effect was much weaker than that of 5 mM Ba^{2+} .

The effects of NDPs

When 3 mM UDP was included in the pipette solution, a significant inward current slowly developed at a holding potential of -70 mV (Figure 4a). The UDP-induced inward current reached its maximum amplitude in 4–10 min, (82 ± 15 pA in 3 mM UDP, $n=5$; 45 ± 10 pA in 0.3 mM UDP, $n=5$) was sustained for more than 20 min and was sensitive to glibenclamide. It was of interest to examine whether or not other NDPs (such as GDP and ADP) evoked the inward current. To minimize the inter-myocytes variation we tested each NDP on cells from the same animal under the same conditions and the maximum amplitude of the inward current was measured (Figure 4a,c). These inward currents were all abolished by glibenclamide ($5 \mu\text{M}$). When $100 \mu\text{M}$ levcromakalim was applied after the NDP-induced inward current had reached its maximum value and become stable, an additional large inward current was evoked. This is illustrated for 3 mM ADP in Figure 4b. Figure 4c summarizes the peak amplitude of the inward current for each NDP included in the pipette solution. The order of potency of the NDPs was $\text{UDP} > \text{GDP} > \text{ADP}$. The glibenclamide-sensitivity of the levcromakalim-induced inward current in the presence of NDPs was tested by application of various concentrations of glibenclamide (5 – $100 \mu\text{M}$, Figure 5a). Although $5 \mu\text{M}$ glibenclamide greatly suppressed the levcromakalim-induced current in the absence of UDP (see open column in Figure 5b), the same concentration of glibenclamide was much less effective in the presence of UDP, and a much higher concentrations was needed to suppress the current to the level achieved in the absence of UDP. Figure 5c shows the average of the four ramp currents before and during application of glibenclamide. Similar results were observed when other NDPs (GDP or ADP, 3 mM each) were included in the pipette solution (data not shown). In contrast, application of 5 mM Ba^{2+} suppressed the levcromakalim-induced current to the control level even when 3 mM UDP had been included in the pipette solution at -70 mV (Figure 6).

Effects of glibenclamide on the levcromakalim-induced unitary channel currents in cell-attached configuration

To investigate further the glibenclamide-sensitive current which was evoked by either levcromakalim or intracellular application of NDPs, single-channel recordings were performed in symmetrical 140 mM K⁺ conditions by use of the cell-attached configuration. To minimize the activity of maxi K⁺ channels, single-channel experiments were performed at negative holding potentials (-70 mV) with $[\text{Ca}^{2+}]_o$ buffered at a low level ($< 2 \text{ nM}$), although significant activity of maxi K⁺ channels sometimes occurred. When $100 \mu\text{M}$ levcromakalim was bath applied, a unitary current was evoked (Figure 7a). Figure 7a shows the effects of glibenclamide. The amplitude of the channel (obtained from the all-points amplitude histogram) was 2.9 pA at -70 mV (Figure 7b). The NP_o value of the K⁺ channel was calculated to be 0.12 . Glibenclamide ($1 \mu\text{M}$) suppressed the channel opening without changing the amplitude (control, 2.9 pA; $1 \mu\text{M}$ glibenclamide, 2.9 pA) and the NP_o value was estimated to be 0.01 (Figure 7b). On removal of $1 \mu\text{M}$ glibenclamide, channel opening recovered to the control level (NP_o value, 0.13). A higher concentration of

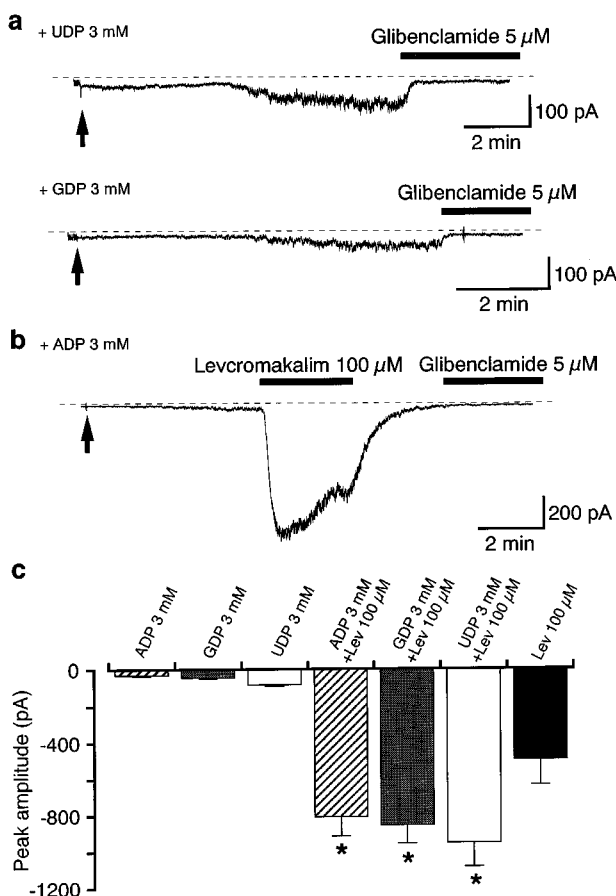


Figure 4 Effects of NDPs on the membrane current in a conventional whole-cell configuration at -70 mV when 3 mM NDP was included in the pipette solution. (a) Effects of either UDP or GDP (3 mM) on the membrane current. Glibenclamide suppressed the 3 mM UDP-induced inward current. Filled arrows indicate the time when a conventional whole-cell configuration was established. The dashed line indicates the zero current level. (b) Effect of $100 \mu\text{M}$ levcromakalim on ADP-induced outward current by use of a conventional whole-cell configuration at -70 mV. When 3 mM ADP was present in the pipette, a small inward current developed slowly after the establishment of the conventional whole-cell configuration (indicated by the filled arrow). Levcromakalim ($100 \mu\text{M}$) caused an additional inward current. The dashed line indicates the zero current level. (c) The peak amplitude of the levcromakalim-induced current with various NDPs (3 mM), in the pipette solution. Currents were measured from the $5 \mu\text{M}$ glibenclamide-sensitive level in each pipette condition. Each column indicates the mean of six observations with s.d. *Significantly different from the peak amplitude of $100 \mu\text{M}$ levcromakalim-induced inward current with no inclusion of NDP (ANOVA, $P < 0.01$).

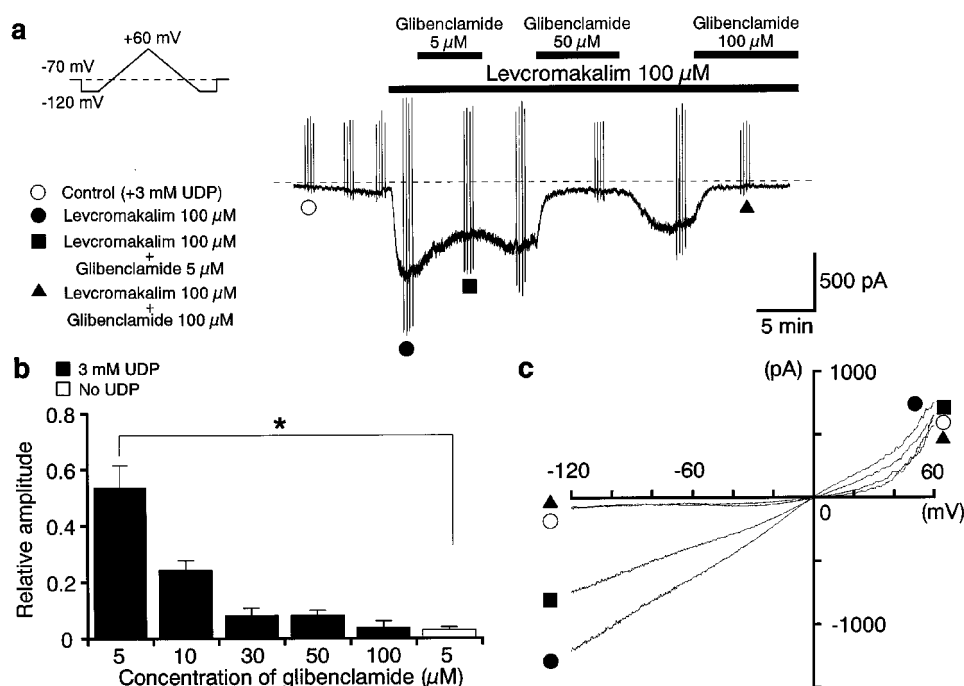


Figure 5 Effects of glibenclamide on the 100 μ M levcromakalim-induced inward current at -70 mV when UDP 3 mM was included in the pipette solution (bath solution, 140 mM K^+ PSS; pipette solution, 140 mM KCl containing 5 mM EGTA). (a) Levcromakalim caused an inward current which was inhibited by additional application of glibenclamide (5, 50 and 100 μ M). Ramp currents induced by the four ramp potential pulses from -120 mV to 60 mV for 900 ms after a 300 ms conditioning pulse (-120 mV, see inset) applied every 15 s before and during application of 100 μ M levcromakalim. The ramp membrane currents were obtained in 140 mM K^+ conditions in the absence (control) and presence of levcromakalim. The vertical deflections indicate ramp currents. The dashed line indicates the zero current level. (b) Relationships between relative inhibition of the peak amplitude of the levcromakalim-induced inward current and the concentration of glibenclamide in the absence (control) and presence of 3 mM UDP. The peak amplitude of the levcromakalim-induced inward current just before applying glibenclamide was normalized as 1.0, measuring from the zero current level. Each symbol indicates the mean with s.d. shown by vertical lines. The current amplitude was significantly different from control ($n=6$), with $P<0.01$ (ANOVA) in the same concentration of glibenclamide (5 μ M). (c) The mean ramp membrane currents on an expanded time scale in several conditions. Each symbol is the same as in (a).

glibenclamide (10 μ M), abolished opening (NP_o value 0). After washing out the 10 μ M glibenclamide, the K^+ channel activity reappeared and recovered to the control level (NP_o value, 0.12). Figure 7c shows the relationships between the NP_o for the 100 μ M levcromakalim-activated K^+ channel and the concentration of glibenclamide at -70 mV ($n=6$). Glibenclamide selectively blocked K^+ channel in a concentration-dependent manner ($K_i=143$ nM).

Inwardly rectifying properties of the glibenclamide-sensitive 40 pS K^+ channel

When the holding potential was changed from -120 mV to 40 mV in the presence of 100 μ M levcromakalim, the conductance, obtained from the amplitude of K^+ channel currents, was 40 ± 3 pS ($n=20$) measured from the all-points amplitude histograms at negative membrane potential (Figure 8). At positive membrane potentials, the $I-V$ relationship demonstrates inward rectification.

UDP-induced reactivation of the K^+ channel in inside-out patches

When the cell-attached patch showed levcromakalim-induced K^+ channel opening at -70 mV, patch excision resulted in a rapid 'run-down' of channel opening in the inside-out configuration, suggesting levcromakalim alone could not sustain channel activity ($n=21$). Figure 9a (i) shows that, after the run-down was complete, application of UDP at a concentration more than 0.1 mM started to reactivate the

2.8 pA K^+ channel in a concentration-dependent manner when 100 μ M levcromakalim was present in the bath. The channel conductance of the UDP-reactivated K^+ channel was 40.4 ± 1.5 pS ($n=8$, data not shown). Other NDPs (such as ADP, GDP, IDP etc. at 3 mM) reactivated the same amplitude K^+ channel in a similar manner (data not shown).

Inhibitory effects of intracellular ATP on the UDP-reactivated K^+ channels

When both 3 mM UDP and 100 μ M levcromakalim were present in the bath, additional application of 0.3 mM ATP to the inner (bath) surface of the membrane patch inhibited opening of the 40 pS K^+ channel (Figure 9b). An increase in the concentration of ATP further reduced the NP_o value. On removal of ATP, the channel opening recovered to the control level.

The shift of the glibenclamide-sensitivity in the UDP-reactivated K^+ channels

As would be expected, additional application of glibenclamide (1–100 μ M) to excised patches showing channel activity in the presence of 3 mM UDP and 100 μ M levcromakalim reversibly inhibited the channel in a concentration-dependent manner, but there was a significant shift of the inhibitory curve to the right ($K_i=4$ μ M, Figure 10b, $n=4$), demonstrating a reduced effectiveness of glibenclamide.

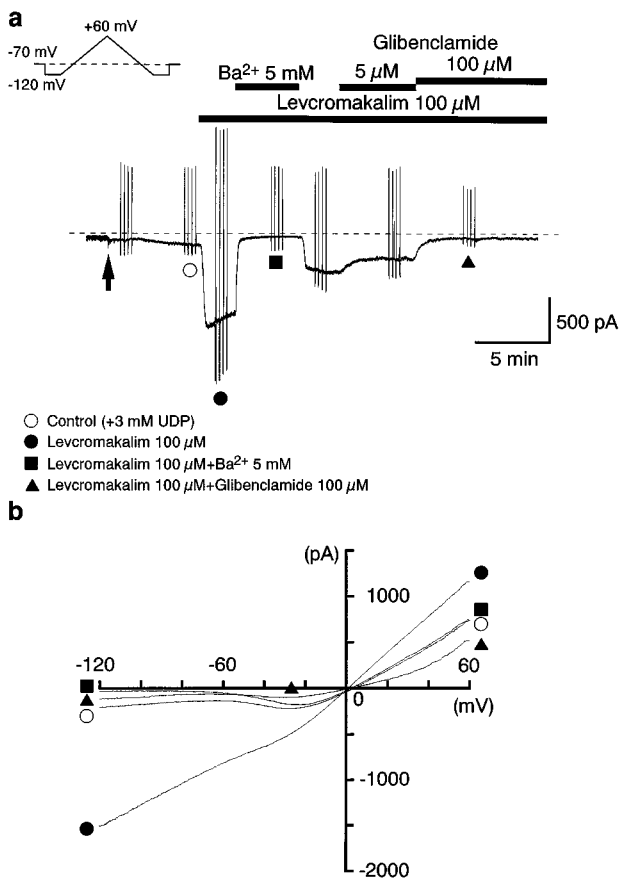


Figure 6 The effects of Ba²⁺ (5 mM) on the 100 μM levcromakalim-induced inward current in comparison with those of glibenclamide (5 μM and 100 μM) at -70 mV when UDP 3 mM was included in the pipette solution (bath solution, 140 mM K⁺ PSS; pipette solution, 140 mM KCl containing 5 mM EGTA). (a) Ramp currents induced by the four ramp potential pulses from -120 mV to 60 mV for 900 ms after a 300 ms conditioning pulse (-120 mV, see inset) applied every 15 s before (control) and during application of 100 μM levcromakalim. The vertical deflections indicate ramp currents. The dashed line indicates the zero current level. (b) The mean ramp membrane currents on an expanded time scale in several conditions. Each symbol is the same as in (a).

Discussion

In the present experiments, we have demonstrated that both levcromakalim and NDPs induce a glibenclamide-sensitive K⁺ current in cat tracheal myocytes, that this current flows through K⁺ channels with a 40 pS conductance, that UDP is capable of reactivating this channel activity in the inside-out configuration and that the glibenclamide-sensitivity was shifted in the presence of 3 mM UDP.

Similarities and differences between the properties of ATP-sensitive K⁺ currents in swine and cat tracheal myocytes

In swine tracheal myocytes, Nuttle & Farley (1997) have described a (±)-cromakalim-induced K⁺ current which was inhibited by intracellular ATP (i.e. K_{ATP} current). However, the current possesses some different properties to the levcromakalim-induced K⁺ current in cat tracheal myocytes. (1) We have been able to demonstrate a significant inwardly rectifying property of the levcromakalim-induced K⁺ currents in cat tracheal myocytes at positive membrane potentials, both in whole cell and single channel recordings. In contrast, the

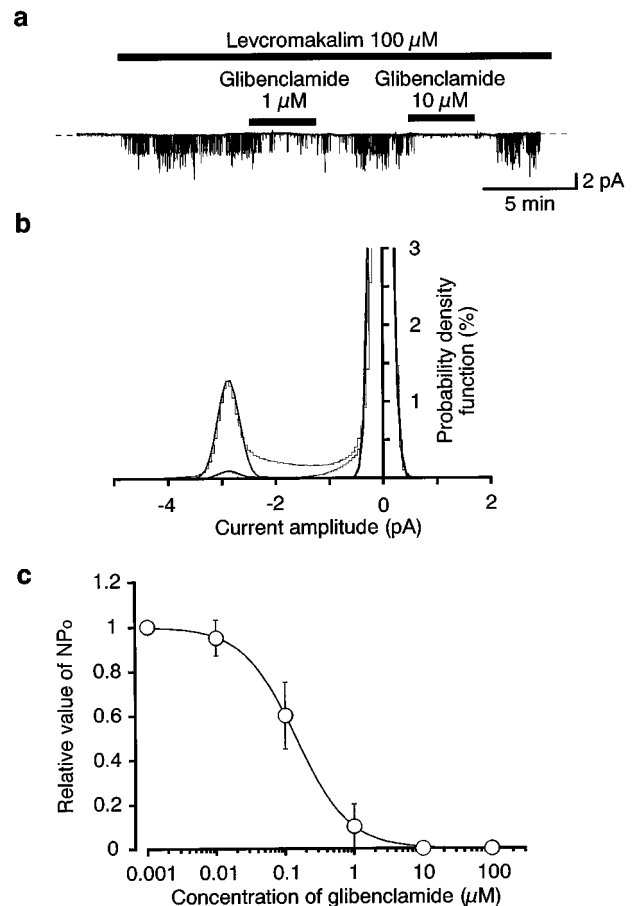


Figure 7 Effects of glibenclamide on the 100 μM levcromakalim-induced 2.9 pA channel at a holding potential of -70 mV. Both 100 μM levcromakalim and glibenclamide were applied in the bath (symmetrical 140 mM K⁺ conditions). Each concentration of glibenclamide was applied for 5 min. (a) Current traces at the indicated concentration of glibenclamide are shown. The dashed line indicates the current base line where the channel is not open. (b) The all-point amplitude histogram for 1 μM glibenclamide was obtained during the last 2 min of a 4 min application. The all-point amplitude histograms were superimposed in the absence (control; just before the application of each concentration of glibenclamide) or presence of glibenclamide (1 μM). Continuous lines in the histograms are theoretical curves fitted with the Gaussian distribution, by the least-squares method. The abscissa scale shows the amplitude of the current (pA) and the ordinate scale shows the percentage value of the probability density function (%) for recording period (2 min). (c) Relationships between relative inhibition of the NP₀ value for the levcromakalim-induced channel and the concentration of glibenclamide. The NP₀ value just before applying glibenclamide was normalized as 1.0. The curve was drawn by fitting the equation using the least-squares method,

$$\text{Relative value of } NP_0 = 1 / \{1 + (K_i / D)^{n_H}\}$$

where K_i , D and n_H are inhibitory dissociation constant, concentration of glibenclamide (nM) and Hill's coefficient, respectively. The following values were used for the curve fitting: $K_i = 143$ nM, $n_H = 1.1$ ($n = 6$). Each symbol indicates the mean with s.d. shown by vertical lines.

current-voltage relationship of the cromakalim-induced membrane current in swine trachea was linear. (2) In cat trachea, much higher concentrations of K_{ATP} opener were required to cause a maximum membrane current (levcromakalim, 100 μM) in comparison with that of swine trachea ((±)-cromakalim, 10 μM). (3) In cat trachea, the levcromakalim-induced K⁺ current was suppressed by additional application of 5 μM glibenclamide in a conventional whole-cell configuration. On the other hand, application of a higher concentration of

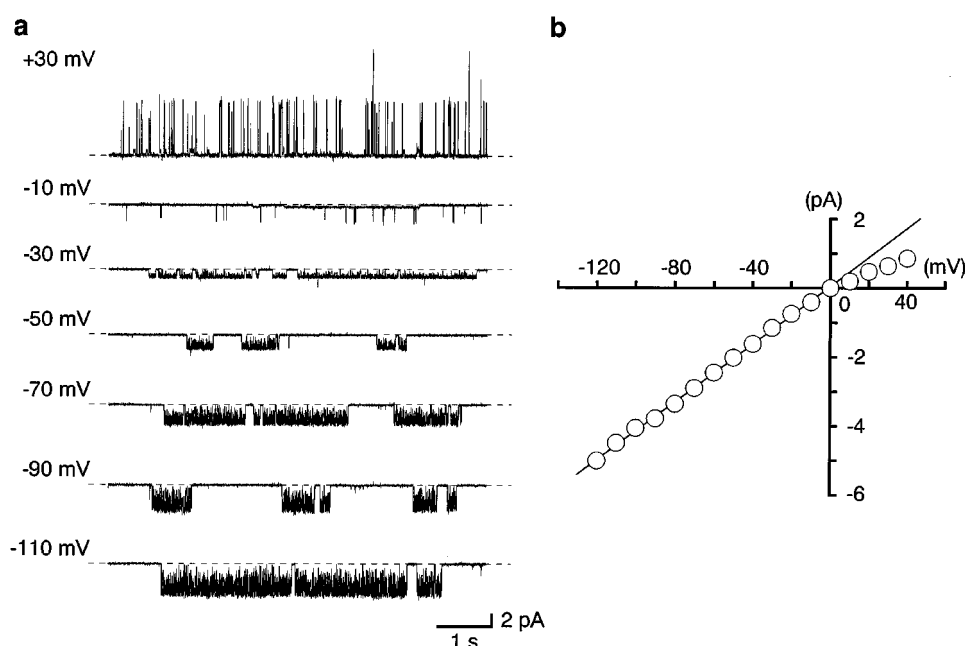


Figure 8 Relationship between the holding membrane potential and the amplitude of the single-channel current activated by $100 \mu\text{M}$ levcromakalim in symmetrical $140 \text{ mM } K^+$ conditions. (a) Traces are channel activities recorded from the same patch membrane at the indicated membrane potentials. The dashed line indicates the current base line where the channel is not open. (b) Current-voltage relationship obtained using cell-attached patch. The amplitude of the K^+ channel currents was taken from the all-points amplitude histograms for 30 s. The line was fitted by the least-squares method. The channel conductance was 41 pS ($40 \pm 3 \text{ pS}$, $n=20$).

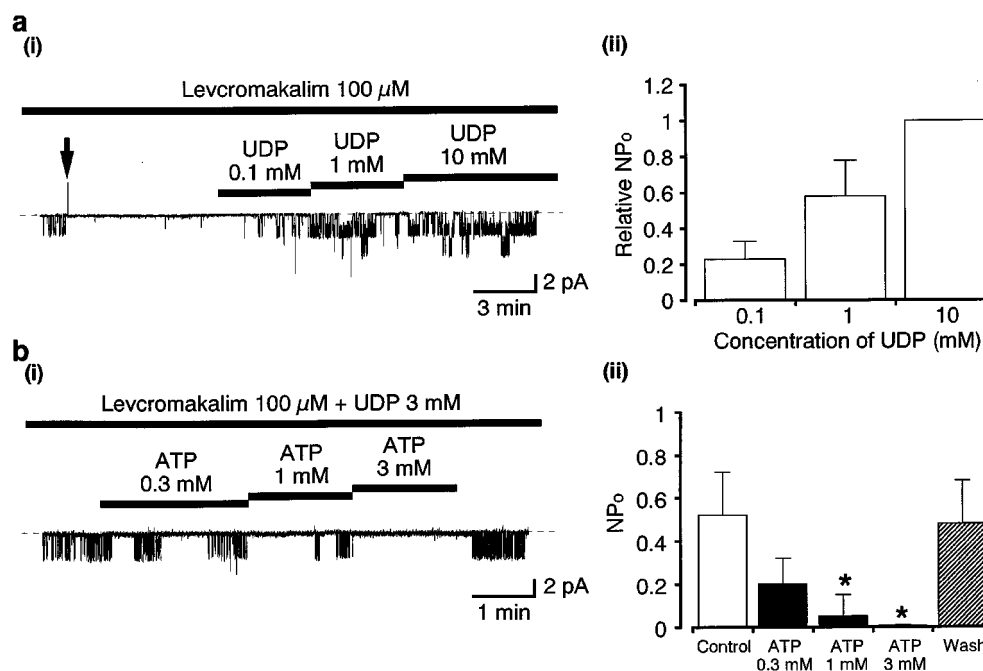


Figure 9 Reactivation of the glibenclamide-sensitive K^+ channel and effects of ATP in inside-out configuration when $100 \mu\text{M}$ levcromakalim was present in the bath solution (symmetrical $140 \text{ mM } K^+$ conditions). The membrane patch was held at -70 mV . (a) (i) When an inside-out patch was established from the cell-attached configuration (excision of the patch membrane at the arrow), the levcromakalim-induced K^+ channel showed a rapid run-down even in the presence of $100 \mu\text{M}$ levcromakalim. Application of 0.1 mM UDP to the inner surface of the membrane patch reactivated the same amplitude of K^+ channel in a concentration-dependent manner. The dashed line indicates the current base line where the channel is not open. (ii) The channel activity (NP_o) of the 10 mM UDP was normalized as 1.0. The columns indicate the relative NP_o values ($\pm \text{s.d.}$) in each concentration of UDP. (b) (i) The application of ATP to the inner surface of the membrane patch suppressed the UDP-reactivated $40 \text{ pS } K^+$ channel in a concentration-dependent manner. After ATP had been washed out, the channel opening recovered to the control level. (ii) Histogram summarizing the inhibition due to the application of ATP. Each column indicates the NP_o value ($\pm \text{s.d.}$) for control, the indicated concentration of ATP, and after washing out ATP ($n=5$). * Significantly different from the control ($P < 0.01$, t -test).

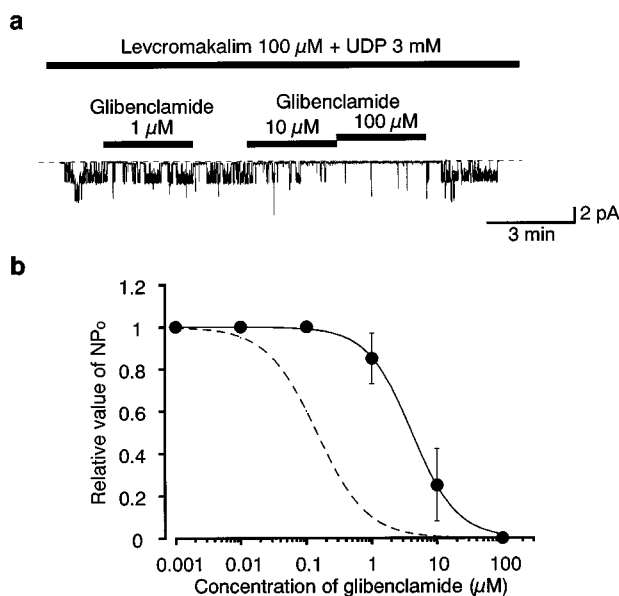


Figure 10 Effects of glibenclamide on the 3 mM UDP-induced channel activity in inside-out configuration when 100 μ M levcromakalim was present in the bath solution (symmetrical 140 mM K⁺ conditions). Each concentration of glibenclamide was applied for 3 min at -70 mV. (a) Current trace at the indicated concentration of glibenclamide (1–100 μ M) is shown. The dashed line indicates the current base line where the channel is not open. (b) Relationships between relative inhibition of the NP_o value for the UDP-activated K⁺ channel and the concentration of glibenclamide. The NP_o value just before applying glibenclamide was normalized as 1.0. The curve was drawn by fitting the equation using the least-squares method,

$$\text{Relative value of } NP_o = 1 / \{1 + (K_i/D)^{n_H}\}$$

where K_i , D and n_H are inhibitory dissociation constant, concentration of glibenclamide (nM) and Hill's coefficient, respectively. The following values were used for the curve fitting: $K_i = 4$ μ M, $n_H = 1.2$ ($n = 4$). Each symbol indicates the mean with s.d. shown by vertical lines. The curve with the broken line was obtained from Figure 7c.

glibenclamide (10 μ M) did not suppress the cromakalim-induced current in swine trachea. Because of the remarkable similarity with respect to intracellular ATP-sensitivity, we are as yet not certain whether these differences may be due to experimental conditions (cultured or freshly dispersed cells, the experimental temperature etc.), or to the different species of smooth muscle.

The glibenclamide-sensitive 40 pS K⁺ channel we have demonstrated in cat tracheal myocytes possesses many properties in common with the glibenclamide-sensitive K⁺ channels seen in other smooth muscle (smooth muscles, Quayle *et al.*, 1997; pig urethra, Teramoto *et al.*, 1997). Namely, (1) Levcromakalim selectively activated the channel. (2) The channel possesses a relatively small conductance (approximately 40 pS) under symmetrical 140 mM K⁺ conditions, demonstrating a significant inwardly rectifying property at positive potentials. (3) Channel run-down was observed when the membrane was excised, even in the presence of K⁺ channel openers. (4) Additional application of NDP caused a reactivation of channel activity even after the run-down of channel activity occurred. (5) The channel activity of this reactivated K⁺ channel was suppressed by ATP which was additionally applied to the inner surface of the excised membrane patches. This glibenclamide-sensitive 40 pS K⁺ channel in cat trachea is the first reported NDP-reactivated ATP-sensitive K⁺ channel in airway smooth muscle cells.

Inhibitory mechanisms of the glibenclamide-sensitive K⁺ channels in cat trachea

In the present experiments, we have been able to compare the time course of the levcromakalim-induced membrane current inhibition evoked by Ba²⁺ and glibenclamide. Since the time course of the inhibitory effect of each blocker could be fitted by a single exponential, it is reasonable to assume that both Ba²⁺ and glibenclamide would each bind to a single site of K_{ATP}. The inhibitory time course of Ba²⁺ was much faster than that of glibenclamide, and this result correlates well with the knowledge that Ba²⁺ applied extracellularly blocks K_{ATP} through binding to a site within the channel pore of inward rectifying K⁺ channels and glibenclamide, one of the most potent sulphonylureas, inhibits K_{ATP} through modulation of sulphonylurea receptors (reviewed by Quayle *et al.*, 1997).

NDP-induced glibenclamide-sensitive K⁺ channels in smooth muscle cells

When NDP was included in the pipette solution, an NDP-induced membrane current was evoked in a conventional whole-cell configuration. Furthermore, the peak amplitude of the levcromakalim-induced membrane current with NDP in the pipette solution was significantly larger than that in the absence of NDP. This remains consistent with the characteristics of the NDP-induced membrane currents reported in other types of smooth muscle cells (rabbit portal vein, Beech *et al.*, 1993; pig urethra, Teramoto *et al.*, 1997). Interestingly, the peak amplitude of the levcromakalim-induced membrane current at -70 mV was gradually reduced when 3 mM ADP was included in the pipette solution in comparison with that of other NDPs. Dunne & Peterson (1986) suggest the possibility that ADP may antagonize the inhibitory effect of ATP on K_{ATP} in the insulin-secreting cell line RINm5F and concluded that the channel opening may be more closely related to the ATP/ADP ratio, than the ATP concentration. Recent molecular expression studies have revealed that the inhibitory potency of ATP and ADP on the channel activity of inwardly rectifying K⁺ channels (i.e. Kir6.2 Δ C26, a mutant form of Kir6.2 in which the last 26 amino acids were deleted from C-terminus) are not markedly different, concluding that both the β -phosphate and moieties within adenine ring are critical for K_{ATP} inhibition by ATP (Tucker *et al.*, 1998). Further biochemical studies of ADP may cast light upon the regulatory mechanisms of the channel openings in K_{ATP} in cat tracheal myocytes.

Although not only the NDP-induced membrane current but also the levcromakalim-induced membrane current were completely inhibited by application of 5 μ M glibenclamide, much higher concentrations of glibenclamide were required to suppress the levcromakalim-induced membrane current in the presence of NDP in the pipette solution, demonstrating a significant shift of the glibenclamide-sensitivity. Although it has also been reported that the sensitivity toward sulphonylureas in cardiac K_{ATP} can be affected by several factors extrinsic to the channel proteins (such as extreme cellular hypoxia, intracellular proton concentrations and disruption of the cytoskeletal network), the action of NDP has been thought to be a competitive antagonism with sulphonylurea in ventricular myocytes (Weiss & Venkatesh, 1993). However, recently, Brady *et al.* (1998) have described a 'two operative conditions hypothesis' in cardiac K_{ATP} (i.e., the spontaneous operative condition and, after rundown of spontaneous activity, the UDP-induced operative condition). They concluded that each operative condition exhibits a distinct

responsiveness toward inhibitory ligands (including ATP and sulphonylureas). In the present experiments, we found that after the rundown of the levromakalim-induced K⁺ channel, the UDP-reactivated K⁺ channel activity was much less sensitive to glibenclamide. This effect was also seen in a conventional whole-cell configuration when 3 mM UDP also reduced the glibenclamide sensitivity when included in the pipette solution. Recent molecular biological and molecular genetic studies of K_{ATP} have revealed that native K_{ATP} appear to be a complex of a regulatory protein containing the sulphonylurea receptor (SUR)-binding site and an inward-rectifying K⁺ channel (K_{ir}) serving as a pore-forming subunit. Three isoforms of SUR (SUR1, SUR2A and SUR2B) have been cloned and found to possess two nucleotide-binding folds (NBFs). It seems that these NBFs play an essential role in conferring the MgADP and K_{ATP} opener sensitivity to the channel (reviewed by Seino, 1999). Recently, Ueda *et al.* (1999) have reported direct biochemical evidence of cooperative interaction in nucleotide binding of the two NBFs of SUR1, demonstrating that glibenclamide both blocks this cooperative binding of ATP and MgADP and, in cooperation with the MgADP bound at NBF2, causes ATP to be released from NBF1. Thus, interaction between intracellular NDPs and inhibitory ligands of K_{ATP} is somewhat complex. In the present experiments, although there is no significant difference in Ba²⁺-sensitivity whether or not UDP was included in the pipette solution, the glibenclamide-sensitivity was significantly shifted in the presence of UDP. These results suggest that intracellular NDP may modify the binding site of sulphonylureas in SUR but not the K⁺ channel in cat tracheal myocytes.

Clinical implications of the glibenclamide-sensitive K⁺ channel in tracheal smooth muscle cells

In the present experiments, we have been able to demonstrate the presence of the levromakalim-induced glibenclamide-sensitive 40 pS K⁺ channel (K_{ATP}) in tracheal smooth muscle

cells by use of single-channel recordings. K_{ATP} openers selectively activate the glibenclamide-sensitive 40 pS K⁺ channel, increasing K⁺ permeability which would hyperpolarize the membrane potential, and result in muscle relaxation in airway smooth muscle. Thus, K_{ATP} openers may have a potent clinical benefit for the treatment of chronic obstructive pulmonary diseases including asthma. Furthermore, it has been shown that K_{ATP} openers inhibit bronchoconstriction mediated by cholinergic (McCaig & De Jonckheere, 1989) and non-adrenergic non-cholinergic (Ichinose & Barnes, 1990) excitatory nerve stimulation. Accordingly, K_{ATP} openers may be useful drugs to control hyperreactivity due to overactive excitatory nerves. However, since the potency of levromakalim for airway smooth muscle is similar to that for vascular and lower urinary tract smooth muscle cells, only local application of K_{ATP} openers would be a useful pharmacological tool for chronic obstructive pulmonary diseases.

In conclusion, we have demonstrated that the levromakalim-induced glibenclamide- and ATP-sensitive K⁺ channels (K_{ATP}) occur in cat tracheal smooth muscle, and can be reactivated by intracellular application of UDP. The presence of intracellular UDP caused a significant shift of the glibenclamide-sensitivity.

We are grateful to SmithKline Beecham Pharmaceuticals for the generous gift of levromakalim (BRL 38227). We are grateful to Prof Alison F. Brading (University, Department of Pharmacology, Oxford) for her helpful discussion and critical reading of the manuscript. This work was supported in part, by the Ministry of Education, Science, Sports and Culture of Japan, Grant-in-Aid (Grant Number 10770042) and Kaibara Morikazu Medical Science Promotion Foundation (Fukuoka, Japan), awarded to Noriyoshi Teramoto.

References

- ALLEN, S.L., BOYLE, J.P., CORTIJO, J., FOSTER, R.W., MORGAN, G.P. & SMALL, R.C. (1986). Electrical and mechanical effects of BRL 34915 in guinea-pig isolated trachealis. *Br. J. Pharmacol.*, **89**, 395–405.
- ARCH, J.R., BUCKLE, D.R., BUMSTEAD, J., CLARKE, G.D., TAYLOR, J.F. & TAYLOR, S.G. (1988). Evaluation of the potassium channel activator cromakalim (BRL 34915) as a bronchodilator in the guinea-pig: comparison with nifedipine. *Br. J. Pharmacol.*, **95**, 763–770.
- BEECH, D.J., ZHANG, H., NAKAO, K. & BOLTON, T.B. (1993). K channel activation by nucleotide diphosphates and its inhibition by glibenclamide in vascular smooth muscle cells. *Br. J. Pharmacol.*, **110**, 573–582.
- BLACK, J.L., ARMOUR, C.L., JOHNSON, P.R., ALOUAN, L.A. & BARNES, P.J. (1990). The action of a potassium channel activator, BRL 38227 (levromakalim), on human airway smooth muscle. *Am. Rev. Respir. Dis.*, **142**, 1384–1389.
- BRADY, P.A., ALEKSEEV, A.E. & TERZIC, A. (1998). Operative condition-dependent response of cardiac ATP-sensitive K⁺ channels toward sulphonylureas. *Circ. Res.*, **82**, 272–278.
- DUNNE, M.J. & PETERSEN, O.H. (1986). Intracellular ADP reactivates K⁺ channels that are inhibited by ATP in an insulin-secreting cell line. *FEBS Lett.*, **208**, 59–62.
- EDWARDS, G. & WESTON, A.H. (1993). The pharmacology of ATP-sensitive potassium channels. *Annu. Rev. Pharmacol. Toxicol.*, **33**, 597–637.
- ICHINOSE, M. & BARNES, P.J. (1990). A potassium channel activator modulates both excitatory noncholinergic and cholinergic neurotransmission in guinea pig airways. *J. Pharmacol. Exp. Ther.*, **252**, 1207–1212.
- MCCAIG, D.J. & DE JONCKHEERE, B. (1989). Effect of cromakalim on bronchoconstriction evoked by cholinergic nerve stimulation in guinea-pig isolated trachea. *Br. J. Pharmacol.*, **98**, 662–668.
- MURRAY, M.A., BOYLE, J.P. & SMALL, R.C. (1989). Cromakalim-induced relaxation of guinea-pig isolated trachealis: antagonism by glibenclamide and by phenolamine. *Br. J. Pharmacol.*, **98**, 865–874.
- NUTTLE, L.C. & FARLEY, J.M. (1997). Muscarinic receptors inhibit ATP-sensitive K⁺ channels in swine tracheal smooth muscle. *Am. J. Physiol.*, **273**, L478–L484.
- QUAYLE, J.M., NELSON, M.T. & STANDEN, N.B. (1997). ATP-sensitive and inwardly rectifying potassium channels in smooth muscle. *Physiol. Rev.*, **77**, 1165–1232.
- SEINO, S. (1999). ATP-sensitive potassium channels: a model of heteromultimeric potassium channel/receptor assemblies. *Annu. Rev. Physiol.*, **61**, 337–362.
- TERAMOTO, N. & BRADING, A.F. (1996). Activation by levromakalim and metabolic inhibition of glibenclamide-sensitive K channels in smooth muscle cells of pig proximal urethra. *Br. J. Pharmacol.*, **118**, 635–642.
- TERAMOTO, N., BRADING, A.F. & ITO, Y. (1999). Glibenclamide-sensitive K⁺ channels underlying levromakalim-induced relaxation in pig urethra. *Eur. J. Pharmacol.*, **365**, 291–300.
- TERAMOTO, N., MCMURRAY, G. & BRADING, A.F. (1997). Effects of levromakalim and nucleoside diphosphates on glibenclamide-sensitive K⁺ channels in pig urethral myocytes. *Br. J. Pharmacol.*, **120**, 1229–1240.

- TUCKER, S.J., GRIBBLE, F.M., PROKS, P., TRAPP, S., RYDER, T.J., HAUG, T., REIMANN, F. & ASHCROFT, F.M. (1998). Molecular determinants of K_{ATP} channel inhibition by ATP. *EMBO J.*, **17**, 3290–3296.
- UEDA, K., KOMINE, J., MATSUO, M., SEINO, S. & AMACHI, T. (1999). Cooperative binding of ATP and MgADP in the sulfonylurea receptor is modulated by glibenclamide. *Proc. Natl. Acad. Sci. U.S.A.*, **96**, 1268–1272.
- WANIISHI, Y., INOUE, R., MORITA, H., TERAMOTO, N., ABE, K. & ITO, Y. (1998). Cyclic GMP-dependent but G-kinase-independent inhibition of Ca²⁺-dependent Cl[−] currents by NO donors in cat tracheal smooth muscle. *J. Physiol.*, **511**, 719–731.
- WEISS, J.N. & VENKETASH, N. (1993). Metabolic regulation of cardiac ATP-sensitive K⁺ channels. *Cardiovasc. Drugs Ther.*, **7**, 499–505.

(Received October 18, 1999

Revised February 4, 2000

Accepted February 29, 2000)